INL/EXT-05-00206

I-NERI Quarterly Technical Progress Report

January 1 – March 31, 2005

Project 2003-013-K – Development of Safety Analysis Codes and Experimental Validation for a Very High Temperature Gas-Cooled Reactor

Chang Oh
Hee Cheon
John Lee
William Martin
James Holloway
Jong Kim
Goon Cherl Park

March 2005

The INL is a U.S. Department of Energy National Laboratory
operated by Battelle Energy Alliance

Idaho National Laboratory

INL/EXT-05-00206

I-NERI Quarterly Technical Progress Report

January 1 – March 31, 2005

Project 2003-013-K – Development of Safety Analysis Codes and Experimental Validation for a Very High Temperature Gas-Cooled Reactor

Chang Oh[a]
Hee Cheon[b]
John Lee[c]
William Martin[c]
James Holloway[c]
Jong Kim[b]
Goon Cherl Park[d]

[a]Idaho National Laboratory
[b]Korea Advanced Institute of Science and Technology
[c]University of Michigan
[d]Seoul National Laboratory

March 2005

Idaho National Laboratory
Idaho Falls, Idaho 83415

Prepared for the
U.S. Department of Energy
Office of Nuclear Energy
Under DOE Idaho Operations Office
Contract DE-AC07-05ID14517

I-NERI QUARTERLY TECHNICAL PROGRESS REPORT

Project Number and Title: Project 2003-013-K, Development of Safety Analysis Codes and Experimental Validation for a Very-High-Temperature Gas-Cooled Reactor

Lead U.S. Investigating Organization: Idaho National Laboratory (INL)
U.S. Principal Investigator: Dr. Chang Oh

Lead Collaborating Investigating Organization: Korea Advanced Institute of Science and Technology (KAIST)
Lead Collaborating Principal Investigator: Prof. Hee Cheon NO

Other Collaborating Organizations:
Profs. John Lee, William Martin, and James Holloway, University of Michigan
Prof. Jong Kim, KAIST
Prof. Goon Cherl Park, Seoul National Laboratory (SNU)

Reporting Period: January 1, to March 31, 2005

Research and Development Areas: Next-generation reactor system

Project Status Summary

The objective of this Korean/United States/laboratory/university collaboration is to develop new advanced computational methods for safety analysis codes for very-high-temperature gas-cooled reactors (VHTGRs) and numerical and experimental validation of these computer codes**.** The research will improve two well-respected light water reactor transient response codes (RELAP5/ATHENA and MELCOR) in the modeling of molecular diffusion and chemical equilibrium, and to validate these codes against the VHTGR accident data, i.e., air ingress and others from the literature. The VHTGR is intrinsically safe, has a proliferation-resistant fuel cycle, and many advantages relative to light water reactors (LWRs). This study consists of five tasks for FY-03: (1) development of computational methods for the VHTGR, (2) theoretical modification of aforementioned computer codes for molecular diffusion (RELAP5/ATHENA) and modeling CO and CO_2 equilibrium (MELCOR), (3) development of a state-of-the-art methodology for VHTGR neutronic analysis and calculation of accurate power distributions and decay heat deposition rates, (4) reactor cavity cooling system experiment, and (5) graphite oxidation experiment.

First quarter of Year 3

- Prof. NO and Kim continued Task 1. We first performed the chemical reaction test for the VELUNA pebble oxidation experiment and then the analysis of the air ingress accident for PBMR 268MWt. In the GAMMA analysis, significant rise in pebble temperature was observed at the bottom of the core due to graphite oxidation. Since the air ingress process depends on the vault conditions, further analysis coupled with more detailed vault or containment modeling would be necessary as a future study.

- Prof. Park continued Task 2. The experiments for SNU-RCCS were continued to provide the experimental data for the validation of the thermal hydraulic code being developed at KAIST and to evaluate the performance of the system using the experiments and system analysis

codes. The three categories of experiments were performed in the facility; 1) upper pool cooling trip test, 2) LOFC experiment, 3) emissivity measurement experiment.

- Prof. NO continued Task 3. (Prof NO) The experimental work of air ingress is going on without any concern: Geometry and size effect test has been completed. The conversion factor for internal surface area was obtained through this experiment. Burn-off test was performed and the uniformity of internal reaction was confirmed.

- INEEL engineers continued to extend the diffusion model for multiple chemical species and made some calculations.

- Prof. Lee and Martin at University of Michigan continued to analyze the effect of the stochastic fuel on the neutronic analysis and have initiated fuel depletion calculations for the VHTGR core. Progress during the past quarter includes:

  Further analysis of stochastic fuel geometry
  Preliminary Monte Carlo depletion of full-core VHTGR
  Installation of MCNP5 on Unix cluster

Narrative:

Task 1:

CFD Thermal Hydraulic Code Development (KAIST)

Task Status and Significant Results

The objective of this task is to develop an analysis tool for thermal-hydraulic transport processes in VHTGR. Thermal hydraulic models to be incorporated in the numerical tool include (1) diffusion of gas species involved, (2) convective mass, momentum, and energy, (3) energy conduction and radiation transport thorough graphite, core barrel, reactor vessel, concrete, and boundary, and (4) heat release by fission and decay heat.

For the analysis of an air ingress accident for a pebble-bed gas-cooled reactor, we selected PBMR 268MWt as a reference reactor because of well-described design information and performed the sensitivity analyses on air volumes in a vault. In order to simulate the chemical reactions during air ingress process, the following chemical reaction models were selected and well tested with the pebble oxidation experiment conducted in the VELUNA test facility [3] as shown at **Fig. 1-1**:

A. CO-O_2 exothermic bulk reaction: [Dryer & Glassmann]

$$R_{CO}\left(kg/m^3-s\right) = -2.24\times10^{12}\exp\left(-167400/\bar{R}T\right)\rho\left(\rho/W_{O_2}\right)^{1/4}\left(\rho/W\right)^{1/2}Y_{CO}Y_{O_2}^{1/4}X_{H_2O}^{1/2}$$

B. C-O_2 exothermic surface reaction: [VELUNA]

$$R_C^{\,w}\left(kg/m^2-hr\right) = 720\exp\left(-16140/T\right)P_{O_2}$$

C. CO_2-C endothermic surface reaction: [Moormann]

$$R_C^{\,w}\left(kg/m^2-s\right)=\frac{0.145\exp\left(-25000/T\right)P_{CO_2}}{1+3.4\times10^{-5}\exp\left(7000/T\right)P_{CO_2}^{\,0.5}}$$

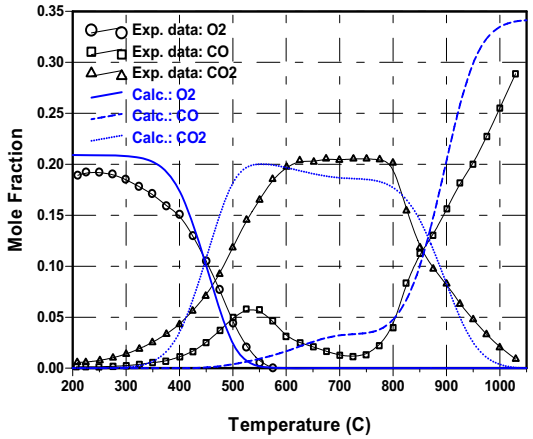

Figure 1-1 Graphite oxidation test for the VELUNA pebble-bed experiment

In PBMR 268MWt, helium at 500°C enters the pebble core through the riser holes and exits at 900°C, at a flow rate of 129 kg/s. **Fig. 1-2** show the GAMMA modeling of PBMR and the helium flow paths at the right figure. The pebble core and reactor cavity are modeled by 2-D geometry, and all the solid structures are modeled by 2-D geometry. For all the cavities or plenums, the radiation heat exchanges are considered.

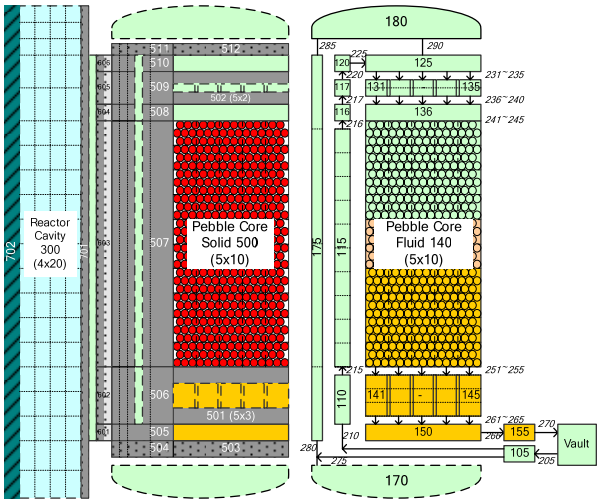

Figure 1-2. GAMMA nodalization for PBMR 268MWt: solid and reactor cavity (left) and fluid component connection (right)

As shown at **Fig. 1-3**, significant rise in pebble temperature was observed at the bottom of the core due to graphite oxidation when the natural convection occurs at about 230 hrs. The

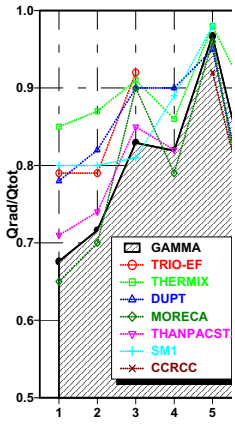

Deleted: Fig. 1 shows the GAMMA nodal scheme for the HTTR-simulated system. The HTTR-simulated experimental facility consisted of a reactor core simulator, a high-temperature plenum, a water-cooled jacket corresponding to the reactor vessel and simulated inlet and outlet pipes to the coaxial pipe. The reactor core simulator has four graphite tubes (one central, #4, and three peripherals, #5) and a ceramic plenum. In order to consider the effect of local natural circulation which promotes air transport through the annular passage, an annular passage (#8) is modeled by 2-D component. Fig. 2 shows the predicted oxygen mole fractions for the non-equal temperature test case (850oC/750oC in central/peripheral graphite tubes). In the first calculation, we have found that the CO2 produced at the bottom region of graphite tubes is trapped in the hot plenum (#3), thereby delaying the onset time of natural convection by about 1.5 days. Its delay is pre... [1]

Formatted ... [2]

Deleted:

Formatted: Justified

Deleted: Fig. 1 shows the GAMMA nodal scheme for the HTTR-simulated system. The HTTR-simulated experimental facility consisted of a reactor core simulator, a high-temperature plenum, a water-cooled jacket corresponding to the reactor vessel and simulated inlet and outlet pipes to the coaxial ... [3]

Formatted ... [4]

sensitivity analyses on air volumes, as shown at **Fig. 1-4**, show that, as air volume decreases, the onset time of natural convection is delayed gradually. However, the peak fuel temperature is not a simple function of air volume but depends on the combination of the bottom reflector temperature and air ingress flow. When the bottom reflector temperature is low, more oxygen survives through the bottom reflector.

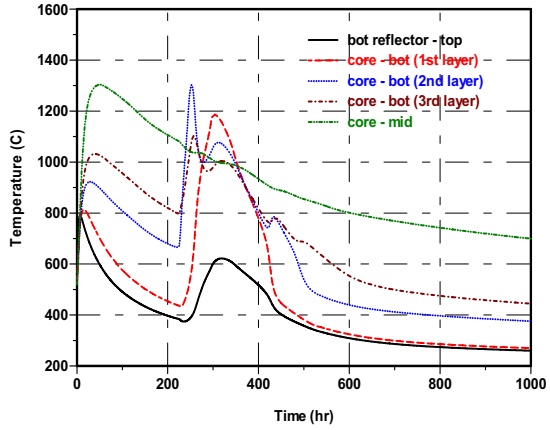

Figure 1-3 Predicted axial temperatures at the center ring (V_{air}=50,000 m^3)

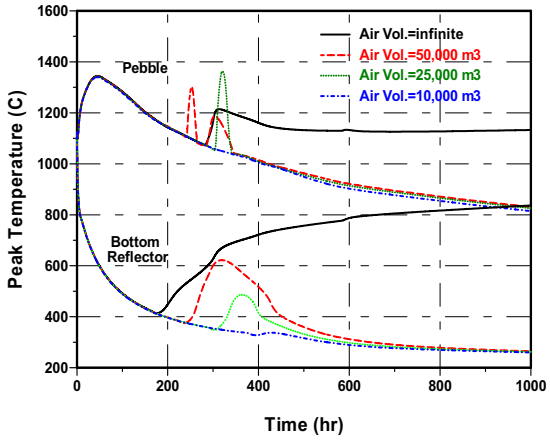

Figure 1-4. Predicted peak fuel temperatures for various air volumes in a vault

Next Quarter Activities

- GT-MHR benchmark calculations for LPCC and HPCC
- Air ingress analysis for the prismatic core GCR (PMR 600MWt)

Issues/Concerns:

There are neither issues nor concerns. This task is right on schedule.

Deleted: Fig. 1 shows the GAMMA nodal scheme for the HTTR-simulated system. The HTTR-simulated experimental facility consisted of a reactor core simulator, a high-temperature plenum, a water-cooled jacket corresponding to the reactor vessel and simulated inlet and outlet pipes to the coaxial pipe. The reactor core simulator has four graphite tubes (one central, #4, and three peripherals, #5) and a ceramic plenum. In order to consider th ... [5]

Formatted: Font: Not Bold, (Asian) Korean, Expanded by 0.05 pt, Not Highlight

Formatted: Font: Not Bold, Expanded by 0.05 pt, Not Highlight

Formatted: Font: Not Bold, (Asian) Korean, Expanded by 0.05 pt, Not Highlight

Formatted: (Asian) Korean, Expanded by 0.05 pt, Not Highlight

Formatted: Expanded by 0.05 pt, Not Highlight

Formatted: Font: Not Bold, Expanded by 0.05 pt, Not Highlight

Formatted: Expanded by 0.05 pt, Not Highlight

Formatted: Not Superscript/ Subscript, Expanded by 0.05 pt, Not Highlight

Formatted: Expanded by 0.05 pt, Not Highlight

Formatted: Not Superscript/ Subscript, Expanded by 0.05 pt, Not Highlight

Formatted: Expanded by 0.05 pt, Not Highlight

Formatted: Not Superscript/ Subscript, Expanded by 0.05 pt, Not Highlight

Formatted: Expanded by 0.05 pt, Not Highlight

Formatted: Font: Not Bold, Expanded by 0.05 pt, Not Highlight

Formatted: Expanded by 0.05 pt, Not Highlight

Formatted: Centered

Deleted: ¶

Task 2:

RCCS Separate Experiment (SNU)

Task Status and Significant Results

The objective of this task is to maintain the structural integrity of the reactor vessel in a completely passive manner by limiting the peak vessel temperature to 427°C and to protect the concrete wall of the cavity. A thorough literature survey was conducted for external and analytical evaluation of gas-cooled reactor cavity cooling system. FY-03 subtask involves development of a water-pool RCCS. We are in progress of performing the following subtasks, which include determination of a proper capacity of water pool to remove decay heat, flow conditions for nonboiling at normal conditions, the effective gap size for the efficient heat removal, and the thickness of the isolation wall.

2.1 Upper pool cooling trip test

The pressure in the upper tank was maintained at atmospheric pressure. As soon as the active cooling is stopped, the temperature of the upper pool increases to the saturation temperature. The temperature near the top of the reactor vessel wall increases as the upper cooling is stopped as shown in **Figure 2-1**. However, it does not increase anymore after the cavity wall temperature reaches the steady state. From this experiment, it was found that the passive cooling capability of the upper pool is sufficient to remove the heat released from the reactor vessel during normal operation. This experimental result will be used to determine the optimized capacity of the water pool.

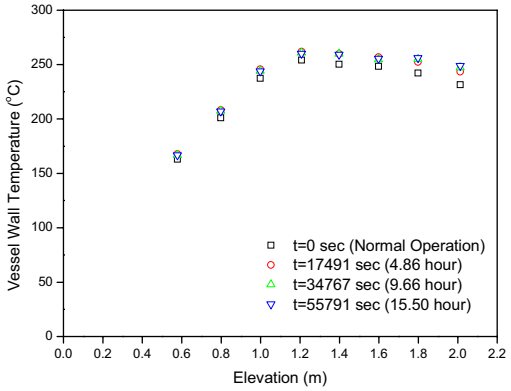

Figure 2-1 Vessel Wall Temperature Transients during Upper Cooling Trip Test

2.2 LOFC experiment

An experiment was carried simulating the LOFC accident, which is the case that the forced convection of the main cooling system of the reactor is failed including the RCCS air coolers. To accentuate the depletion of the side pool and upper pool, the stuck-open of the relief valve was assumed when the water of the side pool reached saturation temperature.

During normal operation, the water pool temperatures were nearly constant along the vertical axis. However, the temperature of the upper part of the water pool increases rapidly with the failure of the entire RCCS active cooling and increase of the heat released from the reactor vessel. After the relief valves were opened at 25,000 second, the upper part temperature in the water pool decreases toward 100℃ and the water level is decreased due to steam generation. As shown in **Figure 2-2**, the cavity wall temperature increased rapidly because incoming heat could not be removed sufficiently at the uncovered region by water.

Figure 2-3 shows the temperature transient of the reactor vessel wall. The temperature increased gradually with the increase of the heat released from the heater. After the heating power was fixed at 40,000 second, most of the region had nearly constant wall temperature. After 60,000 second, however, the area increase of the uncovered cavity wall began to affect the radiative heat transfer from the upper part of the reactor vessel. From this experimental result, we can conclude that 10% of water level reduction by boiling off would be allowed in the water pool type RCCS and this criterion will be applied for the optimization of the system.

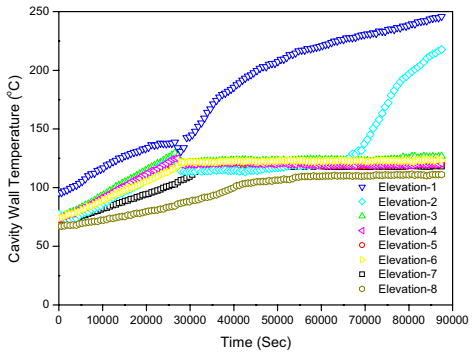

Figure 2-2 Temperature Transients of the Cavity Wall during the LOFC Experiment

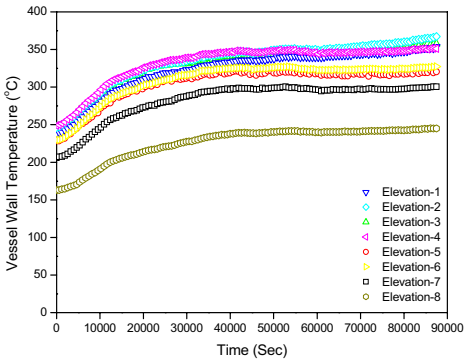

Figure 2-3 Temperature transients of the reactor vessel wall during the LOFC experiment

2.3 Emissivity measurement experiment

The emissivity of the reactor vessel was measured by the infrared thermometer. The sight tube was installed through the water tank and cavity to simplify geometry and facilitate temperature measurement for the calculation. At first, the measured emissivity was compensated by the transmittance of window. Then the effect of background radiation was removed via solving a series of radiative heat transfer equations. This result was compared with the emissivity of same material with reactor vessel of the SNU-RCCS, named true-emissivity in this study, which was measured without any surrounding-surface near the target material in the SET device. As shown in **Figure 2-4**, the calculated emissivity and the true-emissivity emissivity were in a good agreement within the uncertainty band of 3%. Both emissivities gradually increased with temperature at the low temperature range and then approached a constant value as 0.83 around 500 ℃. The result means that the evaluation process is appropriate to predict the effect of background radiation.

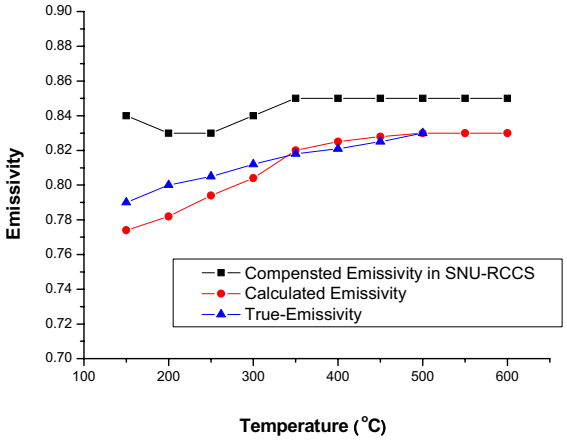

Figure 2-4 comparison of emissivity

Next quarter activities

- The validation and assessment of the safety analysis code such as MARS will continue.
- The optimization of RCCS design using the validated code.

Issues/Concerns:

There are neither issues nor concerns.

Task 3:

Air Ingress Separate Experiment (KAIST)

Task Status and Significant Results

The objective of this task is to carry out graphite oxidation experiment, to determine the oxidation-limited model (chemical kinetics-limited, diffusion-limited or in-pore diffusion-limited model), and to develop measurement techniques of each species' concentration.

A well-defined quantification methodology was developed for geometry and size effects and the conversion factor for internal surface area was obtained here from 16 cases of tests shown in **Figure 3-1**. The internal surface can be calculated as follows:

$$Av = \theta \cdot V ,$$

where Av is an internal surface area, θ is a conversion factor and V is a volume of a graphite material. The calculated θ was 12760. The relative portion of an external reaction to a total reaction was calculated by the following equation and it was illustrated in **Figure 3-2**.

$$I(\%) = \frac{A_s}{A_s + A_v} \times 100 = \frac{A_s}{A_s + \theta \cdot V} \times 100$$

where I is the portion of a external surface reaction and A_s is an apparent surface area. As shown in Figure x, the portion of an external surface area was negligible. **Figure 3-3** shows that the internal reaction uniformly takes place in the inside of a material. The definition of burn-off is as follows:

$$B(\%) = \frac{M_{initial} - M_{final}}{M_{initial}} \times 100 = \frac{\rho_{initial} - \rho_{final}}{\rho_{initial}} \times 100.$$

In this quarter, the chemical regime correlation was completely decided as follows:

$$\frac{R}{V} = r'''(kg/m^3 s) = (A_0 \cdot \theta) \cdot \exp(-\frac{Ea}{R \cdot T}) \cdot P_{O2}{}^n,$$

where,

$$A_0 = 200\ (kg/m^2 s\ Pa^{0.75}),\ \theta = 12760,\ Ea = 218\ (kJ/mol)\ \text{and}\ n = 0.75.$$

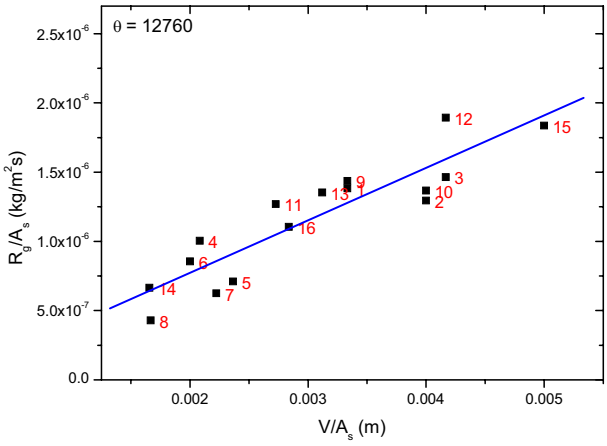

Figure 3-1 Calculation of conversion factor for internal surface area

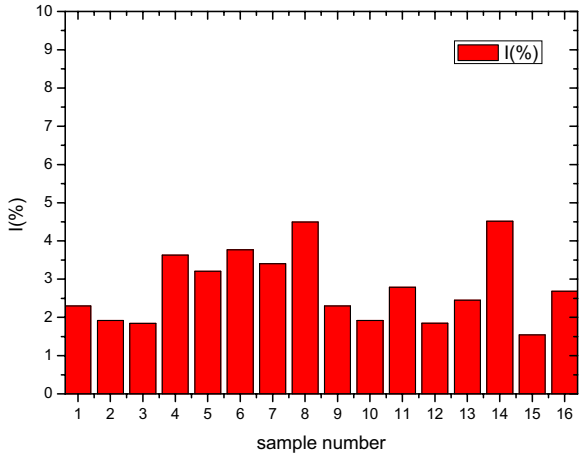

Figure 3-2 Relative portion of external surface reaction to total reaction

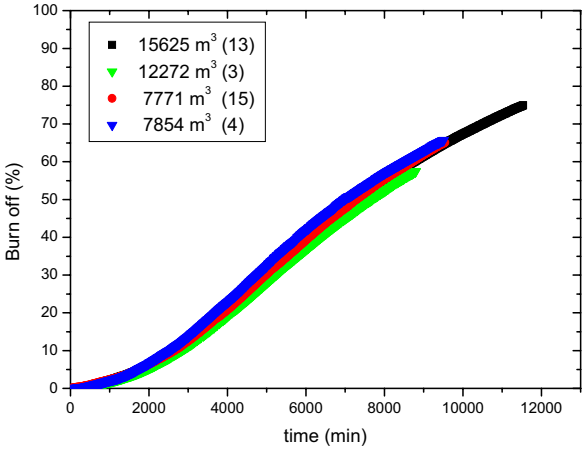

Figure 3-3 Oxidation history for IG-110 graphite in chemical regime

Next quarter activities

- Preparing for moisture effect test
- Finalization of mass transfer test

Issues/Concerns:

There are neither issues nor concerns.

Task 4:

Improvement of System Codes (INL)

Task Status and Significant Results

The objective of this task is to improve the thermal hydraulics system computer codes for analysis of VHGTR systems and to validate these codes against the VHTGR accident data, i.e., air ingress and others from the literature.

The RELAP5/ATHENA code (RELAP5-3D 2002) was extended to model the molecular diffusion of several species of gas through a system represented by a general network of control volumes wherein any control volume can be connected to several other control volumes on its inlet and outlet sides. Previously, the molecular diffusion modeling was applicable only to a gas mixture with two species of gas and only to gas mixture in a pipe wherein each control volume was connected only to one other control volume at each of its two ends. In the extended modeling, the molecular diffusion modeling can be applied to gas mixtures containing up to five species of gas (He, N_2, O_2, CO_2, and CO) and any individual control volume may be connected up to twelve other control volumes on either its inlet or outlet sides.

For a binary mixture of helium and nitrogen in a pipe represented by a single line of control volumes, the explicit scheme numerical equation for the calculating the diffusion through the pipe mixture is (Press et al 1986)

$$\frac{C_i^{n+1} - C_i^n}{\Delta t} = \left[\frac{D_{ip} A_{ip} \left(\frac{C_{i+1}^n - C_i^n}{\Delta x_{ip}} \right) - D_{im} A_{im} \left(\frac{C_i^n - C_{i-1}^n}{\Delta x_{im}} \right)}{\Delta x_i A_i} \right] \tag{1}$$

where

$\frac{C_i^{n+1} - C_i^n}{\Delta t}$ = rate of change of molar concentration of nitrogen in control volume "i" at time step "n+1/2" (1/s),

C_i^n = mole fraction of nitrogen at spatial coordinate in control volume "i" at time step "n" (unitless),

$D_{ip} = 0.5\left(D_i + D_{i+1}\right)$,

$D_{im} = 0.5\left(D_i + D_{i-1}\right)$,

$A_{ip} = \min(A_i, A_{i+1})$,

$A_{im} = \min(A_i, A_{i-1})$,

$\Delta x_{ip} = 0.5\left(\Delta x_i + \Delta x_{i+1}\right)$,

$\Delta x_{im} = 0.5\left(\Delta x_i + \Delta x_{i-1}\right)$,

D_i = diffusion coefficient for a mixture of helium and nitrogen for control volume with index "i" (m^2/s),

A_i = cross-sectional area of control volume with index "i" (m^2),

Δx_i = length of control volume with index "i" (m),

i-1 = index for control volume on outlet side of control volume with index "i",

i+1= index for control volume on inlet side of control volume with index "i".

For a complex network of control volumes and for control volumes with three or more species of gas, the numerical equation for modeling diffusion contains several more terms identifying the various species of gases in the mixture and identifying the various connecting control volumes. The transient concentration of the various species of gas in such a network is calculated by the equation

$$\frac{C_{ji}^{n+1} - C_{ji}^{n}}{\Delta t} = \left[\frac{\sum_{k=1}^{k\max} D_{jik} A_{ik} \left(\frac{C_{jk}^{n} - C_{ji}^{n}}{\Delta x_{ik}} \right) - \sum_{m=1}^{m\max} D_{jim} A_{im} \left(\frac{C_{ji}^{n} - C_{jm}^{n}}{\Delta x_{im}} \right)}{\Delta x_i A_i} \right] \tag{2}$$

where

C_{ji}^{n} = mole fraction of j-th species of gas in control volume "i" at time step "n" (unitless),

k = index identifying one of the RELAP5 control volumes on outlet side of control volume "i",

kmax = total number of RELAP5 control volumes connected to outlet side of control volume "i",

m = index identifying one of the RELAP5 control volumes on inlet side of control volume "i",

mmax = total number of RELAP5 control volumes connected to inlet side of control volume "i",

D_{jik} = effective binary diffusivity of the j-th species of gas in the gas mixture in the diffusion path between control volumes "i" and "k" (m^2/s),

$D_{jik} = \left(\Delta x_i D_{ji} + \Delta x_k D_{jk}\right) / \left(\Delta x_i + \Delta x_k\right)$,

$D_{jim} = \left(\Delta x_i D_{ji} + \Delta x_m D_{jm}\right) / \left(\Delta x_i + \Delta x_m\right)$,

A_{ik} = cross-sectional area for diffusion path between control volumes "i" and "k" (m^2),

$A_{ik} = \min(A_i, A_k)$,

$A_{im} = \min(A_i, A_m)$,

Δx_{ik} = length of diffusion path between control volumes "i" and "k" (m),

$\Delta x_{ik} = 0.5\left(\Delta x_i + \Delta x_k\right)$,

$\Delta x_{im} = 0.5\left(\Delta x_i + \Delta x_m\right)$.

The effective binary diffusivity of the j-th species of gas in the gas mixture can be calculated by the equation (Reid et al. 1986)

$$D_{jg} = \left(\sum_{n=1, n\neq j}^{n\max} \frac{x_n}{D_{jn}} \right)^{-1} \tag{3}$$

where

D_{jg} = effective binary diffusivity of the j-th species of gas in the gas mixture (m^2/s),

nmax = number of species of gas in the gas mixture (unitless),

x_n = mole fraction of n-th species of gas in the gas mixture (unitless),

D_{jn} = binary diffusivity of the j-th and n-th species of gas (m^2/s).

The binary diffusivity for the j-th and n-th species of gas is calculated by the correlation (Reid et al. 1986, RELAP5-3D 2002)

$$D_{jn} = \frac{0.0101325\left(\frac{1.}{w_j}+\frac{1.}{w_n}\right)^{0.5} T_{ig}^{1.75}}{\left[P_{ig}\left\{a_{dj}^{0.333}+a_{dn}^{0.333}\right\}^{2.0}\right]} \quad (4)$$

where

T_{ig} = temperature of gas mixture in control volume with index "i" (K),

P_{ig} = pressure of gas mixture in control volume with index "i" (Pa),

w_j = molecular weight of j-th species of gas in gas mixture,

w_n = molecular weight of n-th species of gas in gas mixture,

a_{dj} = atomic diffusion volume for j-th species of gas in gas mixture,

a_{dn} = atomic diffusion volume for n-th species of gas in gas mixture.

The atomic diffusion volumes for each species of gas are defined in the RELAP5/ATHENA subroutine named rnoncn.

A simple but rigorous test problem was constructed to assess for internal consistency the modeling extensions for gas mixtures containing several species of gas in a general network of control volumes. The test problem involved the calculation of the transient mixing together in a pipe of four species of gas originally separated from each other. The calculation was performed with two different nodalizations that should produce identical results for correct modeling of a general network of control volumes. In the first nodalization, the gas mixture in the pipe is represented by a single row of four equally sized control volumes. This nodalization is shown in Figure 1. In the second nodalization of the pipe, multiple connections were applied to the outlet side of control volume 101 and to the inlet side of control volume 104 shown in Figure 1. This nodalization is shown in Figure 2. For the nodalization shown in Figure 1, control volumes with identification numbers of 101 and 102 initially contain a mixture of N_2, O_2, and CO_2 at a pressure of 0.1 MPa and a temperature of 291 K. The initial mass fractions of N_2, O_2, and CO_2 in these control volumes were 0.769, 0.1, and 0.131, respectively. These gases are the "non-working" fluid. The control volumes with identification numbers of 103 and 104 initially contain He (the working fluid) at a pressure of 0.1 MPa and a temperature of 291 K. The length of each of the four control volume is 0.1 m and the control volumes are equal in cross-sectional area. At the time of zero seconds, the valve isolating control volumes 101 and 102 from control volumes 103 and 104 is fully opened (cross-sectional area of opened valve equal to the cross-sectional area of the four control volumes) and the various species of gas begin to mix together. In the second nodalization of the pipe, control volumes 102 and 103 in Figure 1 were each split into two equally sized control volumes with the sum of the cross-sectional area of each of these two pairs

equal to the cross-sectional area of the pipe shown in Figure 1. For this nodalization, control volumes 102 and 104 represent one half of the middle section of the pipe and control volumes 103 and 105 the other half. The outlet side of control volume 101 is connected to both control volumes 102 and 103 and the inlet side of control volume 106 is connected to both control volumes 104 and 105. The cross-sectional area of the pipe is everywhere the same as for the pipe shown in Figure 1. Control volumes 101, 102, and 103 initially contain the same mixture of N_2, O_2, and CO_2 as the control volumes 101 and 102 in Figure 1, and control volumes 104, 105, and 106 initially contain He at the same conditions as that in control volumes 103 and 104 in Figure 1.

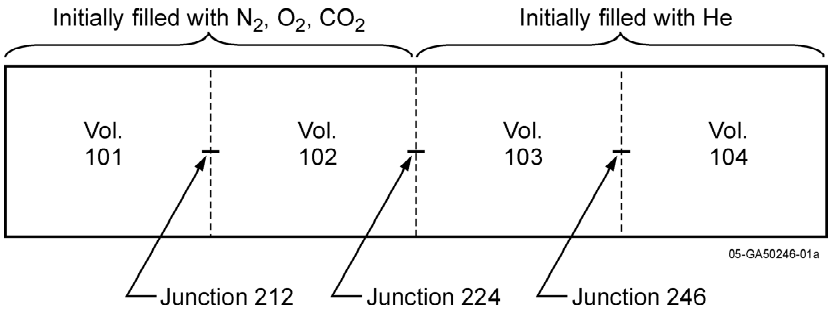

Figure 1. Nodalization of pipe containing a mixture of gases as a single row of four equally sized control volumes.

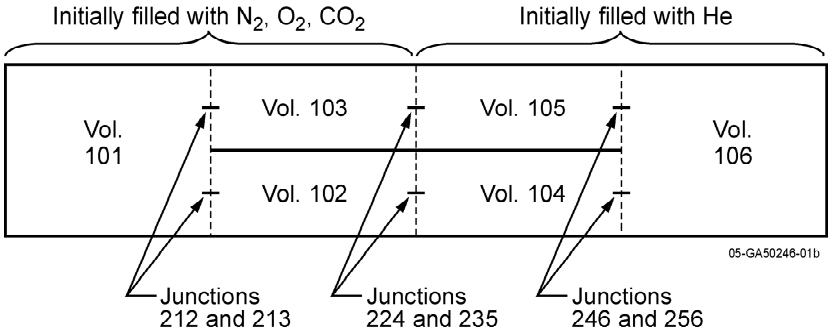

Figure 2. Nodalization of pipe with control volumes at ends of pipe having multiple connections to inlet or outlet side.

The calculations performed with the nodalization shown in Figure 1 were found to be identical with the calculations performed using the nodalization shown in Figure 2. Figure 3 compares the transient mass fraction of the non-working gases (N_2, O_2, and CO_2) at the two ends of the pipe as calculated for the case with single connections in the control volumes at the two ends of the pipe and for the case with multiple connections in the control volumes at the two ends of the pipe. A mass fraction of zero in a control volume corresponds with that control volume only containing helium (the working fluid). As shown in this figure, the results for the two nodalizations are identical; the curves for the multiple junction case lie within the curves for the single junction case. For correct modeling, the calculations should predict that the mass fractions of the non-working gases (N_2, O_2, and CO_2) at the opposite ends of the pipe asymptotically approach the same value. Figure 3 shows that this requirement of modeling is also met. In

summary, the results shown in Figure 3 indicate that the extensions made to the RELAP5/ATHENA code for modeling a generalized network of control volumes and gas mixtures with several species of gas have been correctly implemented.

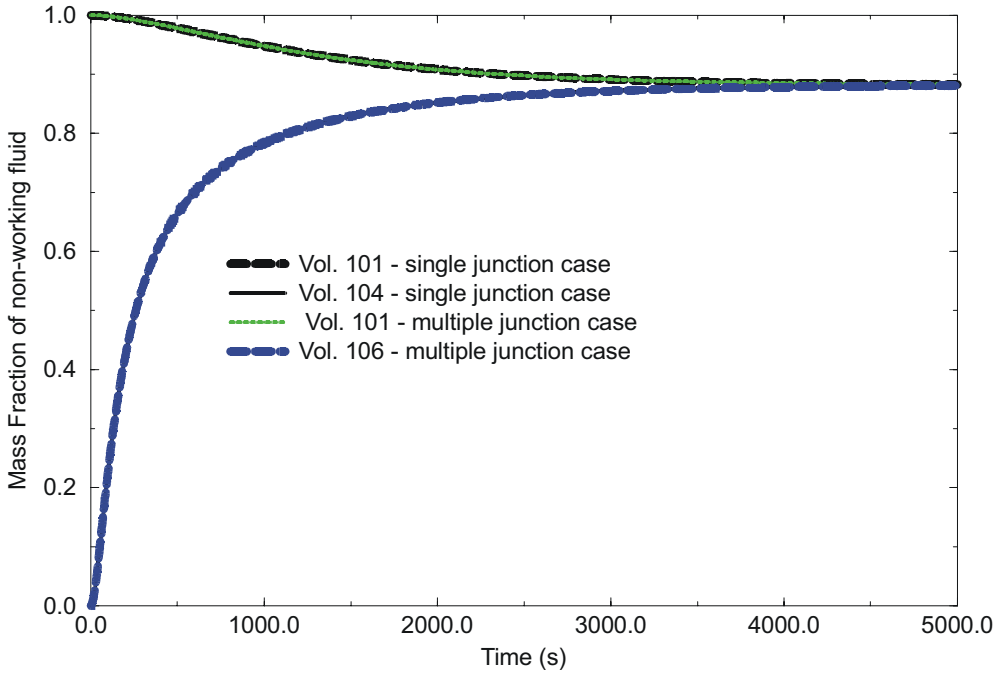

Figure 3. Transient concentration of non-working fluid gases (N_2, O_2, and CO_2) at the two ends of pipe.

Next Quarter Activities

- Interface modeling of chemical reactions in HTGR core with extensions for modeling of diffusion of several species of gas.
- Analyze conduction cooldown accident in Pebble Bed HTGR with application of extensions in modeling of gas diffusion and chemical reactions in the core.

References

Press et al. 1986 — W. H. Press et al., **Numerical Recipes**, Cambridge University Press, New York, NY, 1986.

Reid et al. 1986 — R. C. Reid, J. M. Prausnitz, and B. E. Poling, *The Properties of Gases and Liquids*, Fourth Edition, McGraw-Hill Book Company, New York, 1986.

RELAP5-3D 2002 — The RELAP5-3D-3D Development Team, *RELAP5-3D-3D Code Manual*, INEEL-EXT-98-00834, Revision 2.0, July 2002.

Next quarter activities

-More diffusion validation will be performed.

Issues/Concerns:

No issues or concerns.

Task 5:

Neutronic Modeling (University of Michigan)

Task Status and Significant Results

The objective of this task is to develop a state-of-the-art neutronics model for determining power distributions and decay heat deposition rates in a VHTGR core. We have made progress during the past quarter on (a) further analysis of stochastic fuel geometry, (b) preliminary Monte Carlo depletion of full-core VHTGR, and (c) installation of MCNP5 on a Unix cluster

Stochastic fuel geometry

Previous results have shown that the 2-region model (fuel kernel; fuel coatings and graphite matrix) yields acceptable results compared with the 6-region model when the microspheres are located on a lattice. We have extended this analysis to geometries with microspheres randomly placed in a fuel compact cell, consisting of a fuel compact (a right circular cylinder of length 4.928 cm and diameter 1.245 cm) surrounded by its share of the graphite portion of a fuel block, as depicted in Figure 1 below. The following cases were analyzed:

Case 1 – The fuel region consists of 5-region microsphere cells randomly placed in a fuel compact (graphite matrix) using random sequential addition (RSA) in each of 50 layers. This "stratified RSA" method results in 129 heterogeneous microspheres (fuel kernel and 4 coatings) being inserted into each of the 50 layers in the fuel compact. This is a "6-region" fuel configuration. See Figure 1.

Case 2 – Same as Case 1 except the microsphere coatings are mixed with the graphite matrix and the fuel kernels are placed at the identical points as the full microspheres. This is a "2-region" fuel configuration.

Case 3 – Same as Case 1 except RSA is performed in 10 layers rather than 50 layers, resulting in more random placement of the microspheres. See Figure 2.

Case 4 – Same as Case 2 except 10 layers.

The results for Cases 1-4 are given in Table 1. These results confirm that the 2-region microsphere cell yields acceptable results for particle fuel where the microspheres are randomly located within a finite geometry as well as located on a lattice as we had previously reported. The effect of implementing RSA in 50 layers versus 10 layers appears to be negligible, but this is still under examination.

Table 1. MCNP5 Simulations of Fuel Compact Cells

Case	# regions	# layers	# realizations	k_{eff}	Sigma
1*	2	50	2	1.34237	.00022
2*	6	50	2	1.34268	.00022
3	2	10	19	1.34228	.00019
4	6	10	2	1.34258	.00022

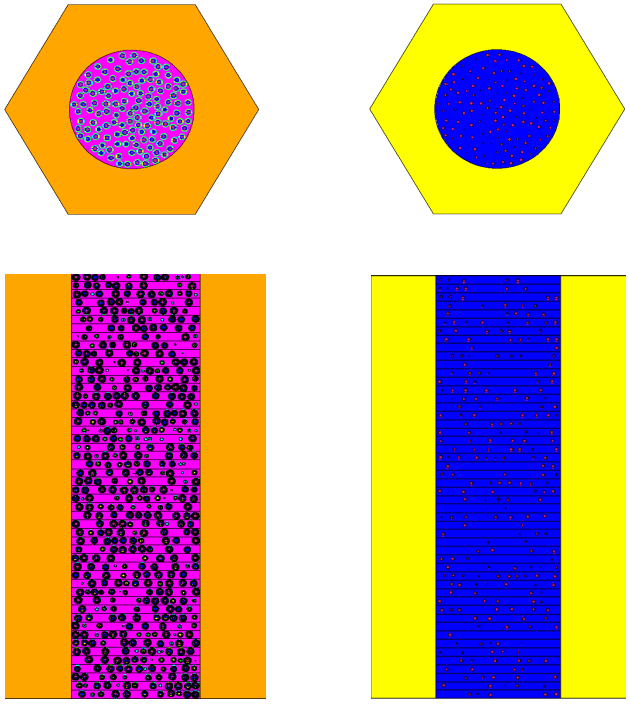

Figure 1. MCNP5 Fuel Compact Geometries:
Six-region (left) and Two-region (right) Stochastic (RSA) Configurations

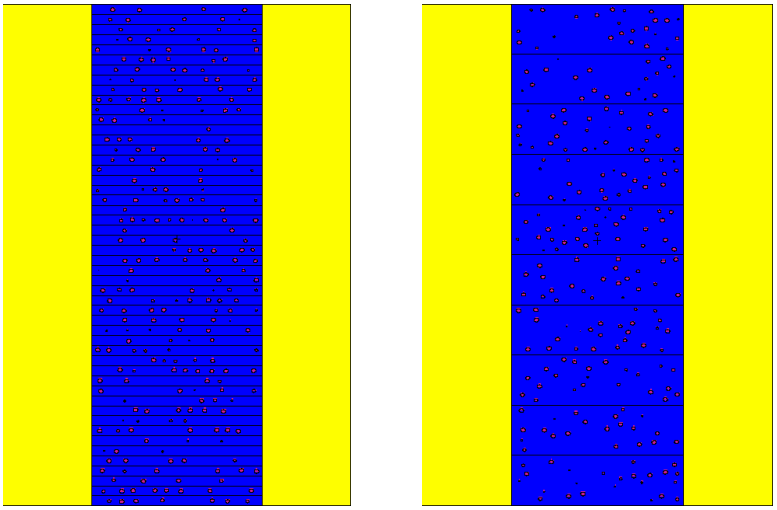

Figure 2. MCNP5 Fuel Compact Geometries:
Fifty-layer (left) and Ten-layer (right) Configurations

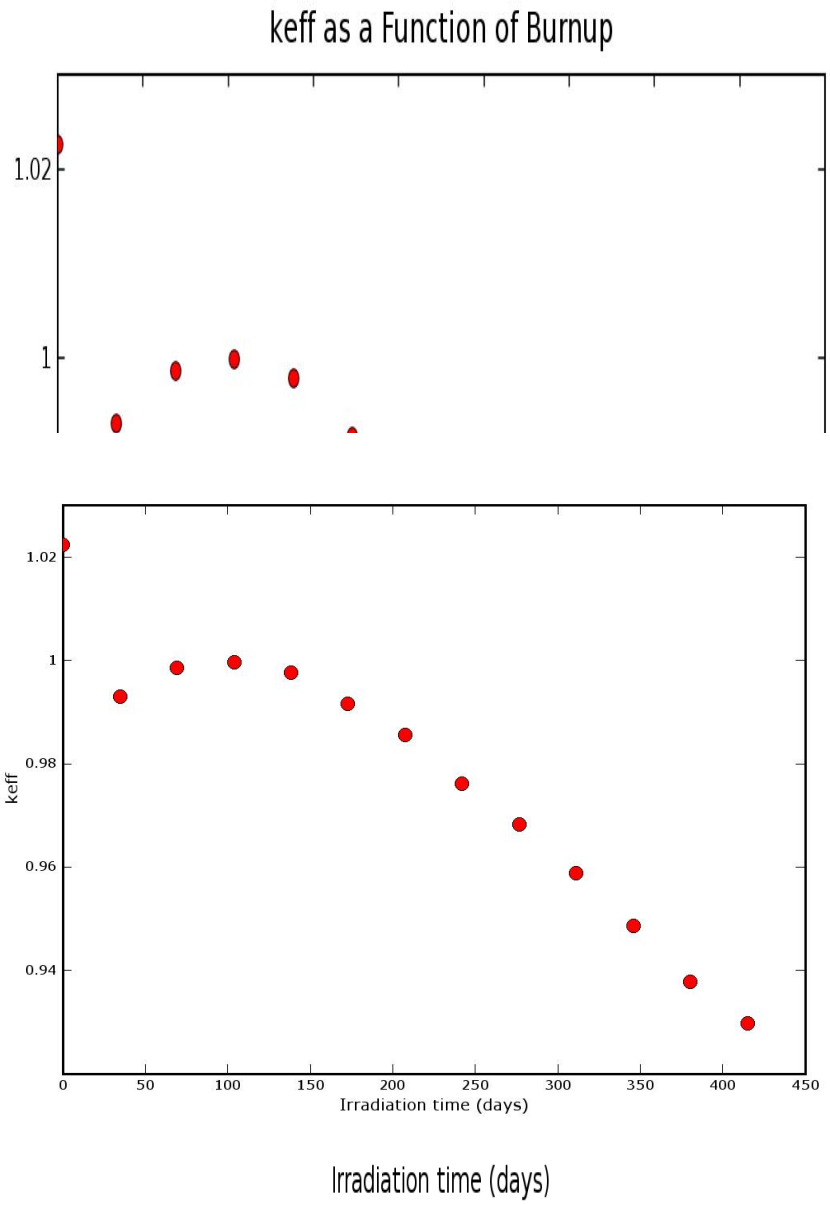

Installation of MCNP5 on Unix cluster

A Macintosh G5 cluster has been installed and is operational in the department. MCNP5 has been installed and is operational on this cluster. There are five servers in the cluster, four compute nodes and one head node. Each server has dual 2.5GHz G5 CPUs. A Cisco Gigabit Ethernet switch makes this cluster very efficient for parallel applications such as production MCNP runs. We have obtained a speedup of 7.9 using eight CPUs for MCNP5 analyses. We have also installed MCNP5 on a larger G5 cluster (128 CPUs) that is operated by the Center for Advanced Computing (CAC) in the College of Engineering. We expect these clusters will be very helpful for our MCNP5 depletion runs using Monteburns and for coupled neutron-photon transport calculations.

Effort in Next Quarter

- Perform whole-core fuel depletion calculations accounting for 3-D power distributions in the core and initiate coupled neutron-photon transport calculations for decay heat analysis.
- Consider an alternative method to avoid clipping of the microspheres that preserves the packing fraction but does not result in a non-cubical microsphere cell.

Task 6:

V&V Simulation (INEEL and KAIST)

The V&V simulations for GAMMA are summarized in the following **Table 6-1**. The part A including 14 simulation cases has been finished. We are now performing the plant applications (B1 and B2) of the GAMMA code to PBR and PMR.

Table 6-1 Assessment matrix for the GAMMA code

No.	Test Facility	Phenomenon	Remarks
A. Code V&V			
A1	Pipe Network, North West University	Flow balancing in a complex pipe network	2 cases
A2	Blowdown, North West University	Pressure transient Critical flow	2 cases
A3	Duncan & Toor's experiment	Multicomponent molecular diffusion	
A4	Inverse U-tube single/multiple channel	Binary molecular diffusion and natural convection	1 isothermal test 2 non-isothermal tests 4 multiple channel tests
A5	Ogawa's circular tube	Chemical reactions in a IG-110	
A6	Takahashi's annular tube	Chemical reactions in a IG-110	
A7	VELUNA pebble bed	Chemical reactions in a pebble bed	
A8	Inverse U-tube air ingress experiment	Molecular diffusion, natural convection, and chemical reactions	10 He-N2 cases 11 He-Air cases including 1 isothermal case
A9	HTTR-simulated air ingress experiment	Molecular diffusion, natural convection, and chemical reactions Multi-D effect on air ingress process	15 equal/non-equal temperature cases
A10	Vertical slot experiment	Local circulation effect on molecular diffusion	
A11	NACOK natural convection test	Natural convection in a pebble bed	Air and air-he mixture
A12	SANA-1 afterheat removal test	Pebble temperature distributions: Steady power tests Power ramp up/down tests	14 steady power cases 4 power ramp cases
A13	HTTR RCCS mockup te	Air convection and radiation in a reacto	7 cases

	st	r cavity	
A14	SNU RCCS test	Air convection and radiation in a reacto r cavity	6 cases
B. Plant Application			
B1	PBR air ingress analysis	LPCC with air ingress for a pebble-bed core gas-cooled reactor	
B2	PMR air ingress analysis	LPCC with air ingress for a prismatic c ore gas-cooled reactor	

Project Milestone/Deliverable Summary:

Milestone/Deliverable Description	Planned Completion	Actual Completion
1. CFD TH Code Development	30 June 2005	In progress
1-1 CFD TH model	31 December 2004	Completed
1-2 Diffusion model	31 December 2003	Completed
1-3 Chemical reaction model	30 June 2005	In progress
1-4 Particle model	30 June 2005	In progress
2. RCCS Separate Experiment	30 June 2005	In progress
2-1. Development of water-pool RCCS	31 December 2003	Completed
2-2. Scaling of water-pool RCCS	30 June 2004	Completed
2-3 Heat transfer coefficients	30 June 2005	In progress
3. Air Ingress Separate Experiment	30 June 2005	In progress
3-1. Measurement technique development	30 June 2004	Completed
3-2. Diffusion-limited model	30 June 2005	In progress
4-1. Implementation of Diffusion model	31 May 2005	In progress
4-1-A. Noncondensable gas implementation	30 April 2003	Completed
4-1-B Diffusion model	31 December 2003	Completed
4-1-C Simulation	31 July 2005	In progress
4-2. Implementation of Chemical Equilibrium Model	31 December 2003	Completed
4-2-A. Simulation	31 July 2005	In progress
5. Neutronic Modeling	31 December 2005	In Progress
6. V&V Simulation	31 December 2005	In progress
6-1. RCCS validation	31 December 2005	In progress
6-2. System code vs. CFD code	31 December 2005	In progress
6-3. Large-scale air ingress analysis	31 December 2005	Starts in Year-3
6-4. System-scale simulation	31 December 2005	Starts in Year-3

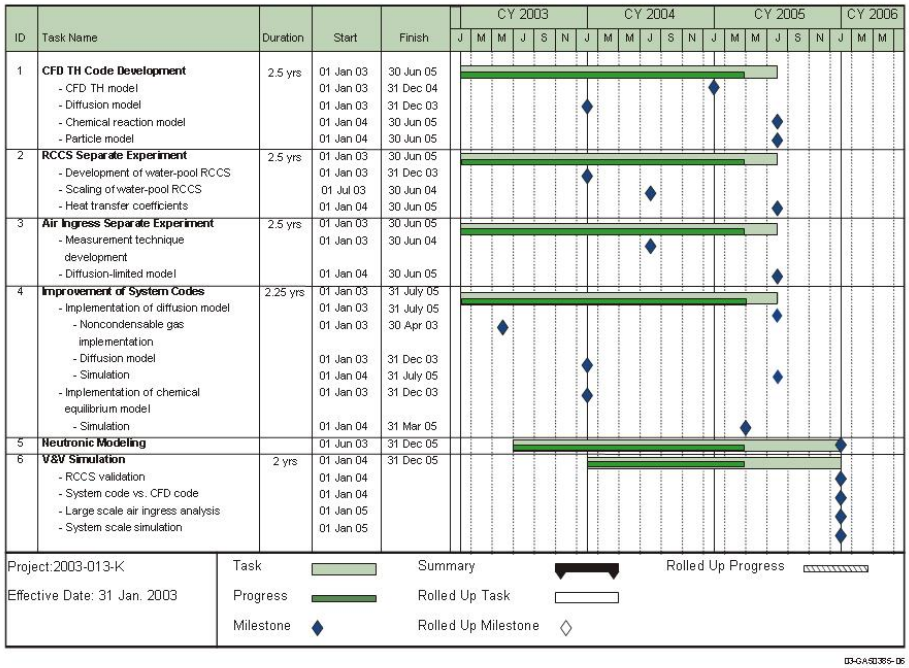
ID
Task Name
Duration
Start
Finish
CY 2003
CY 2004
CY 2005
CY 2006
J M M J S N J M M J S N J M M J S N J M M
1 CFD TH Code Development 2.5 yrs 01 Jan 03 30 Jun 05
- CFD TH model 01 Jan 03 31 Dec 04
- Diffusion model 01 Jan 03 31 Dec 03
- Chemical reaction model 01 Jan 04 30 Jun 05
- Particle model 01 Jan 04 30 Jun 05
2 RCCS Separate Experiment 2.5 yrs 01 Jan 03 30 Jun 05
- Development of water-pool RCCS 01 Jan 03 31 Dec 03
- Scaling of water-pool RCCS 01 Jul 03 30 Jun 04
- Heat transfer coefficients 01 Jan 04 30 Jun 05
3 Air Ingress Separate Experiment 2.5 yrs 01 Jan 03 30 Jun 05
- Measurement technique development 01 Jan 03 30 Jun 04
- Diffusion-limited model 01 Jan 04 30 Jun 05
4 Improvement of System Codes 2.25 yrs 01 Jan 03 31 July 05
- Implementation of diffusion model 01 Jan 03 31 July 05
- Noncondensable gas implementation 01 Jan 03 30 Apr 03
- Diffusion model 01 Jan 03 31 Dec 03
- Simulation 01 Jan 04 31 July 05
- Implementation of chemical equilibrium model 01 Jan 03 31 Dec 03
- Simulation 01 Jan 04 31 Mar 05
5 Neutronic Modeling 01 Jun 03 31 Dec 05
6 V&V Simulation 2 yrs 01 Jan 04 31 Dec 05
- RCCS validation 01 Jan 04
- System code vs. CFD code 01 Jan 04
- Large scale air ingress analysis 01 Jan 05
- System scale simulation 01 Jan 05
Project:2003-013-K
Effective Date: 31 Jan. 2003
Task
Progress
Milestone
Summary
Rolled Up Task
Rolled Up Milestone
Rolled Up Progress
03-GA50385-05

Page 3: [1] Deleted	Hong Sik Lim	9/15/2004 5:40:00 PM

Fig. 1 shows the GAMMA nodal scheme for the HTTR-simulated system. The HTTR-simulated experimental facility consisted of a reactor core simulator, a high-temperature plenum, a water-cooled jacket corresponding to the reactor vessel and simulated inlet and outlet pipes to the coaxial pipe. The reactor core simulator has four graphite tubes (one central, #4, and three peripherals, #5) and a ceramic plenum. In order to consider the effect of local natural circulation which promotes air transport through the annular passage, an annular passage (#8) is modeled by 2-D component. Fig. 2 shows the predicted oxygen mole fractions for the non-equal temperature test case (850oC/750oC in central/peripheral graphite tubes). In the first calculation, we have found that the CO2 produced at the bottom region of graphite tubes is trapped in the hot plenum (#3), thereby delaying the onset time of natural convection by about 1.5 days. Its delay is presumed to be caused by several internal leak paths, which are established directly as well as indirectly through the thermal insulator (#7) from the hot side to the cold side. Therefore, in the subsequent calculation, all the leak paths are modeled by single path (#13) with a very small flow area. The predicted results considering an internal leak path show better agreement with the experimental data than that without a leak path. For all experimental cases simulated, Fig. 3 shows that the onset times of natural convection are accurately predicted within a 10% deviation.

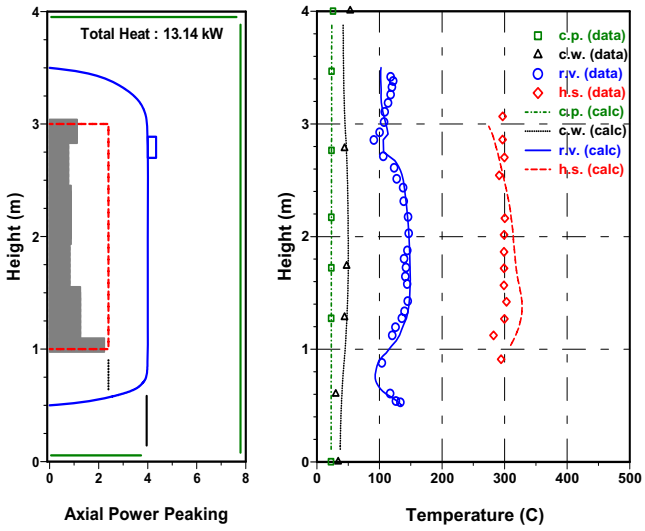

Page 3: [2] Formatted	Hong Sik Lim	9/15/2004 5:43:00 PM

Font: Not Bold, Not Highlight

Page 3: [2] Formatted	Hong Sik Lim	9/15/2004 5:43:00 PM

Font: Not Bold, Not Highlight

Page 3: [2] Formatted	Hong Sik Lim	9/15/2004 5:43:00 PM

Font: Not Bold, Not Highlight

Page 3: [2] Formatted	Hong Sik Lim	9/15/2004 5:43:00 PM

Not Highlight

Page 3: [2] Formatted	Hong Sik Lim	9/15/2004 5:43:00 PM

Not Highlight

Page 3: [2] Formatted	Hong Sik Lim	9/15/2004 5:43:00 PM

Font: Not Bold, Not Highlight

Page 3: [2] Formatted	Hong Sik Lim	9/15/2004 5:43:00 PM

Not Highlight

Page 3: [2] Formatted	Hong Sik Lim	9/15/2004 5:43:00 PM

Not Superscript/ Subscript, Not Highlight

Page 3: [2] Formatted	Hong Sik Lim	9/15/2004 5:43:00 PM

Not Highlight

Page 3: [2] Formatted	Hong Sik Lim	9/15/2004 5:43:00 PM

Not Superscript/ Subscript, Not Highlight

Page 3: [2] Formatted	Hong Sik Lim	9/15/2004 5:43:00 PM

Not Highlight

Page 3: [2] Formatted	Hong Sik Lim	9/15/2004 5:43:00 PM

Not Superscript/ Subscript, Not Highlight

Page 3: [2] Formatted	Hong Sik Lim	9/15/2004 5:43:00 PM

Not Highlight

Page 3: [2] Formatted	Hong Sik Lim	9/15/2004 5:43:00 PM

Font: Not Bold, Not Highlight

Page 3: [2] Formatted	Hong Sik Lim	9/15/2004 5:43:00 PM

Not Highlight

Page 3: [3] Deleted	Hong Sik Lim	9/15/2004 5:40:00 PM

Fig. 1 shows the GAMMA nodal scheme for the HTTR-simulated system. The HTTR-simulated experimental facility consisted of a reactor core simulator, a high-temperature plenum, a water-cooled jacket corresponding to the reactor vessel and simulated inlet and outlet pipes to the coaxial pipe. The reactor core simulator has four graphite tubes (one central, #4, and three peripherals, #5) and a ceramic plenum. In order to consider the effect of local natural circulation which promotes air transport through the annular passage, an annular passage (#8) is modeled by 2-D component. Fig. 2 shows the predicted oxygen mole fractions for the non-equal temperature test case (850oC/750oC in central/peripheral graphite tubes). In the first calculation, we have found that the CO2 produced at the bottom region of graphite tubes is trapped in the hot plenum (#3), thereby delaying the onset time of natural convection by about 1.5 days. Its delay is presumed to be caused by several internal leak paths, which are established directly as well as indirectly through the thermal insulator (#7) from the hot side to the cold side. Therefore, in the subsequent calculation, all the leak paths are modeled by single path (#13) with a very small flow area. The predicted results considering an internal leak path show better agreement with the experimental data than that without a leak path. For all experimental cases simulated, Fig. 3 shows that the onset times of natural convection are accurately predicted within a 10% deviation.

Page 3: [4] Formatted	Hong Sik Lim	9/15/2004 5:43:00 PM

Font: Not Bold, (Asian) Korean, Expanded by 0.05 pt, Not Highlight

Page 3: [4] Formatted	Hong Sik Lim	9/15/2004 5:43:00 PM

Font: Not Bold, Expanded by 0.05 pt, Not Highlight

Page 3: [4] Formatted	Hong Sik Lim	9/15/2004 5:43:00 PM

Font: Not Bold, (Asian) Korean, Expanded by 0.05 pt, Not Highlight

Page 3: [4] Formatted	Hong Sik Lim	9/15/2004 5:43:00 PM

(Asian) Korean, Expanded by 0.05 pt, Not Highlight

Page 3: [4] Formatted	Hong Sik Lim	9/15/2004 5:43:00 PM

Expanded by 0.05 pt, Not Highlight

Page 3: [4] Formatted	Hong Sik Lim	9/15/2004 5:43:00 PM

Font: Not Bold, Expanded by 0.05 pt, Not Highlight

Page 3: [4] Formatted	Hong Sik Lim	9/15/2004 5:43:00 PM

Expanded by 0.05 pt, Not Highlight

Page 3: [4] Formatted	Hong Sik Lim	9/15/2004 5:43:00 PM

Not Superscript/ Subscript, Expanded by 0.05 pt, Not Highlight

Page 3: [4] Formatted	Hong Sik Lim	9/15/2004 5:43:00 PM

Expanded by 0.05 pt, Not Highlight

Page 3: [4] Formatted	Hong Sik Lim	9/15/2004 5:43:00 PM

Not Superscript/ Subscript, Expanded by 0.05 pt, Not Highlight

Page 3: [4] Formatted	Hong Sik Lim	9/15/2004 5:43:00 PM

Expanded by 0.05 pt, Not Highlight

Page 3: [4] Formatted	Hong Sik Lim	9/15/2004 5:43:00 PM

Not Superscript/ Subscript, Expanded by 0.05 pt, Not Highlight

Page 3: [4] Formatted	Hong Sik Lim	9/15/2004 5:43:00 PM

Expanded by 0.05 pt, Not Highlight

Page 3: [4] Formatted	Hong Sik Lim	9/15/2004 5:43:00 PM

Font: Not Bold, Expanded by 0.05 pt, Not Highlight

Page 3: [4] Formatted	Hong Sik Lim	9/15/2004 5:43:00 PM

Expanded by 0.05 pt, Not Highlight

Page 3: [4] Formatted	Hong Sik Lim	9/15/2004 5:43:00 PM

Font: 11 pt, Expanded by 0.05 pt

Page 4: [5] Deleted	Hong Sik Lim	9/15/2004 5:40:00 PM

Fig. 1 shows the GAMMA nodal scheme for the HTTR-simulated system. The HTTR-simulated experimental facility consisted of a reactor core simulator, a high-temperature plenum, a water-cooled jacket corresponding to the reactor vessel and simulated inlet and outlet pipes to the coaxial pipe. The reactor core simulator has four graphite tubes (one central, #4, and three peripherals, #5) and a ceramic plenum. In order to consider the effect of local natural circulation which promotes air transport through the annular passage, an annular passage (#8) is modeled by 2-D component. Fig. 2 shows the predicted oxygen mole fractions for the non-equal temperature test case (850oC/750oC in central/peripheral graphite tubes). In the first calculation, we have found that the CO2 produced at the bottom region of graphite tubes is trapped in the hot plenum (#3), thereby delaying the onset time of natural convection by about 1.5 days. Its delay is presumed to be caused by several internal leak paths, which are established directly as well as indirectly through the thermal insulator (#7) from the hot side to the cold side. Therefore, in the subsequent calculation, all the leak paths are modeled by single path (#13) with a very small flow area. The predicted results considering an internal leak path show better agreement with the experimental data than that without a leak path. For all experimental cases simulated, Fig. 3

shows that the onset times of natural convection are accurately predicted within a 10% deviation.